

Coding Agents with Environment Interaction: A Theoretical Perspective

Nicolas Menet^{1,2} Michael Hersche¹ Andreas Krause² Abbas Rahimi¹

Abstract

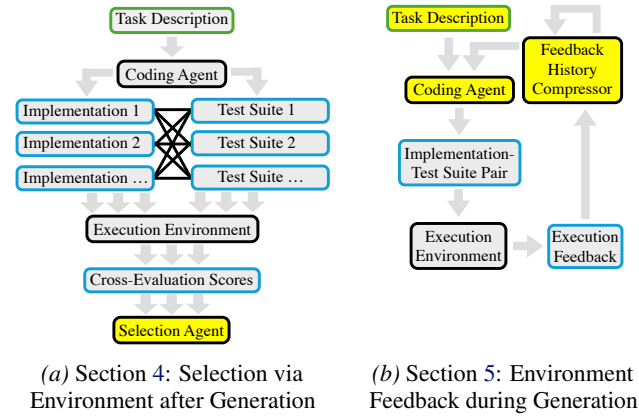
Coding agents are increasingly utilized in test-driven software development, yet the theoretical mechanisms behind their environment-interaction strategies remain underexplored. We provide a probabilistic framework for two dominant paradigms: code selection after generation using the execution environment, and code generation conditioned on environment feedback. First, we formalize several well-established selection heuristics as environment-aware estimators of code correctness. We theoretically prove that estimators based on fuzzy functional similarity add an inductive bias and strictly dominate estimators based on functional equivalence in terms of signal-to-noise ratio. Second, we frame backprompting as an in-context approximation of Thompson sampling. We derive a novel regret bound for reward functions with unobservable components, theoretically explaining why the effectiveness of backprompting is limited by the ambiguity of the informal task description (an irreducible regret). Using three state-of-the-art open weight models, we corroborate these findings across BigCodeBench-Hard, LeetCodeDataset, and QiskitHumanEvalSim. Our formalization also suggests how to improve task descriptions effectively, leading to a new benchmark, QiskitHumanEvalSimX.

1. Introduction

Large Language Models (LLMs) have demonstrated strong capabilities across several domains (OpenAI, 2023), including code assistants (Chen et al., 2021). These code assistants have quickly been integrated into disruptive products, such as Github Copilot, Claude Code, and Cursor.

With code assistants increasingly adopted for critical large-scale software, their capability to conduct test-driven development (Beck, 2003) becomes paramount. In addition to

¹IBM Research Zurich, Zürich, Switzerland ²Department of Computer Science, ETH Zurich, Zürich, Switzerland. Correspondence to: Nicolas Menet <menetn@ethz.ch>.



(a) Section 4: Selection via Environment after Generation

(b) Section 5: Environment Feedback during Generation

Figure 1. We consider coding agents with environment interaction in two settings: post-generation selection via self-evaluation (left, Section 4) and in-the-loop backprompting of execution feedback (right, Section 5). Our contributions are highlighted in yellow.

facilitating collaboration and quality control, test-driven development provides a unique opportunity for boosting LLM performance via post-generation selection (Li et al., 2022; Shi et al., 2022; Chen et al., 2023) or iterative backprompting (Shinn et al., 2023; Olausson et al., 2024; Chen et al., 2024c). Environment-aware post-generation selection leverages test suites to score implementations and group equally (or similarly) behaving code. In contrast, backprompting of execution results provides the language model with an opportunity to refine its own beliefs on the behavior of code. These strategies are illustrated in Figure 1. Although widely used, their theoretical mechanisms remain underexplored.

In this work, we adopt a probabilistic perspective on both types of environment interaction. Our contributions are as follows: (1) We formalize post-generation selection heuristics as estimators of environment-aware probability of correctness, introducing a unifying categorization of prior works in Table 1. We prove that estimators adopting functional similarity add an inductive bias that diminishes neural approximation artifacts and strictly dominate estimators built on functional equivalence in terms of signal-to-noise-ratio. This provides a theoretical basis for why aggregating “similar” behaviors is more robust than counting identical outputs. (2) We explore the limitations of conditioning the LLM on environment feedback during generation. To that end, we frame backprompting as an

in-context approximation of Thompson sampling. We then derive a novel regret bound for reward functions with unobservable components. The bound identifies an irreducible regret: the effectiveness of backprompting is strictly limited by the ambiguity of the task description, regardless of the quantity of execution feedback. (3) We confirm these findings experimentally using three state-of-the-art open weight models (Qwen3-235B-Instruct, GPT-OSS-120B, MiniMax-M2.1) across BigCodeBenchHard, LeetCodeDataset, and QiskitHumanEval. Our results confirm that “soft” estimators (adopting functional similarity) consistently outperform “hard” ones (adopting functional equivalence), and that backprompting is most effective in settings with a small unobservable reward component. Finally, we verify the importance of clear task descriptions for effective backprompting by deriving a novel dataset QISKITHUMANEVALSIMX.

2. Related Work

LLMs for Code Generation Since the introduction of Codex (Chen et al., 2021), a model fine-tuned on GitHub, code generation has become a central application of LLMs. Modern general-purpose models now routinely include substantial code data during training (Qwen Team, 2025).

Post-Generation Selection Strategies Selection heuristics have become dominant for improving performance without retraining (Wang et al., 2023). ALPHACODE (Li et al., 2022) popularized selecting generations based on pass rates on ground-truth tests and behavioral similarity under self-generated inputs. In scenarios where external tests are unavailable, heuristics like MBR-EXEC (Shi et al., 2022) and CODET (Chen et al., 2023) select solutions based on agreement groups—sets of codes that pass the same self-generated tests. Current heuristics, such as CODET, rely on “hard” agreement (counting identical outputs). Our work theoretically formalizes these as environment-aware estimators of program correctness and proposes “soft” estimators that use fuzzy functional similarity to improve accuracy.

Iterative Refinement via Backprompting Beyond selection, environment feedback is used to iteratively refine code. Frameworks like REFLEXION (Shinn et al., 2023) use verbal reinforcement learning, asking LLMs to reflect on textual feedback to guide repairs. Similarly, SELFREPAIR (Olausson et al., 2024) executes a repair step based on external test failures. While these methods assume valid, discriminative tests provided, our framework addresses the more common setting where agents rely on self-generated tests. In this setup, we frame backprompting as approximate Thompson sampling (Thompson, 1933; Russo & Roy, 2014). This allows us to theoretically identify an irreducible regret: a term in the regret bound caused by the inherent task ambiguity.

Bayesian Perspectives on In-Context Learning Recent theoretical work by Xie et al. (2022) and Chlon et al. (2025) demonstrates that in-context learning conducts approximate Bayesian inference. Sutter et al. (2025) argue that pre-training on sequence data with cross-entropy loss naturally yields models capable of Thompson sampling. While Menet et al., (2025b) explore Thompson sampling via fine-tuning of LLMs, we study the emergent Thompson sampling capabilities of off-the-shelf LLMs via in-context conditioning. This allows us to apply regret bounds from Bayesian optimization to explain the limits of backprompting strategies.

3. Preliminaries

Notation Let \mathcal{V} be a finite vocabulary of tokens. For any set Ω , the Kleene star denotes the set of all finite strings $\Omega^* := \cup_{i \geq 0} \Omega^i$. Hence, \mathcal{V}^* represents the space of all possible token strings, including code implementations. We denote the number of test cases in a test suite $t \in \mathcal{V}^*$ by $|t|$.

Problem Setting We assume a generative process driven by a prior distribution over abstract *algorithms* $a \in \mathcal{A}$ and *environments* $e \in \mathcal{E}$ (execution contexts). The environment constrains the available tools (e.g., libraries) and required syntax to implement the algorithm. We observe a natural language task *description* $d \in \mathcal{V}^*$ (the informal specification), which is a lossy compression of the algorithm a and environment e . Crucially, the abstract algorithm a is inherently unobservable beyond d . In contrast, the environment e can be partially observed. Given a description d and an observation history \mathcal{H} , we seek two latent variables: a *test suite* $t \in \mathcal{V}^*$ (the executable specification) that formalizes the requirements of algorithm a in environment e , and an *implementation* $c \in \mathcal{V}^*$ valid under this test suite. We model $p(c, t | \mathcal{H}, d)$ with a large language model and shorten the notation by omitting the dependency on d . Figure 2 represents these dependencies as a structural causal model.

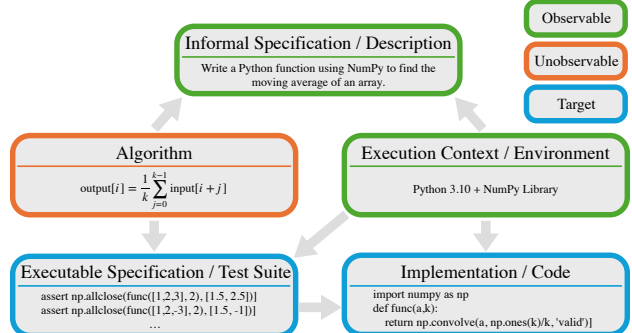


Figure 2. Generative process represented as a structural causal model (arrows indicate causality). We observe an informal specification (description) corresponding to an algorithm in an execution context (environment). We seek an executable specification (test suite) and an implementation that satisfies it (code).

Environment Feedback Given an environment $e \in \mathcal{E}$, code $c \in \mathcal{V}^*$, and test suite $t \in \mathcal{V}^*$, we consider both scalar and textual environment feedback. Let \mathbb{O} be a vocabulary of test outputs. Then, $O(c, t | e) \in \mathbb{O}^{|t|}$ is the direct output of the test harness. Typically, $\mathbb{O} = \{0, 1\}$ with 0 indicating failure and 1 success. In this case, a scalar reward is recovered via $R(c, t | e) := \frac{1}{|t|} \sum_i O_i(c, t | e) \in [0, 1]$. More generally, strategies such as functional consensus rely on generalized test suites with large \mathbb{O} , e.g., corresponding to arbitrary function output. Lastly, more informative textual feedback can be obtained from a test report $U(c, t | e) \in \mathcal{V}^*$, e.g., in the form of captured `stderr` and assertion tracebacks.

Adopting an environment-centric view, we first formalize popular post-generation selection mechanisms that leverage the environment, before examining in-the-loop strategies based on backprompting of environment feedback.

4. Selection via Environment after Generation

Code generation should target the underlying *algorithm* rather than a specific implementation. However, autoregressive next-token prediction leads to probability mass being fragmented unevenly across many functionally identical implementations—an issue known as *program aliasing* (Bunel et al., 2018; Zhong et al., 2018). To remedy such modeling artifacts, selection strategies must operate at an algorithmic granularity that groups equally behaving codes. In this section, we first define key concepts such as functional similarity and functional equivalence. We then use estimators thereof to factor out program aliasing. We analyze their signal-to-noise ratio and conclude that functional similarity is significantly more robust. Finally, we unify several prior works in Table 1. All proofs are in the appendix.

Definition 4.1 (Functional Code Similarity). Given an environment $e \in \mathcal{E}$ and a distribution over test suites $p(t)$, we define the similarity between two implementations c_1, c_2 as

$$\text{sim}_{p,e}(c_1, c_2) := \mathbb{E}_{t \sim p} \left[\frac{1}{|t|} \sum_{k=1}^{|t|} \mathbb{1}_{O_k(c_1, t | e) = O_k(c_2, t | e)} \right],$$

where O_k denotes the output of the k -th test case.

Note that this similarity implicitly depends on the task description d via $p(t)$. This dependency focuses the functional comparison on the intended input domain, diminishing fragmentation due to divergent handling of edge cases undefined by d , and reducing variance of Monte Carlo estimation.

Proposition 4.2 (Kernel Structure of Functional Code Similarity). *The similarity $\text{sim}_{p,e}(c_1, c_2)$ is a positive semi-definite (PSD) kernel with $\text{sim}_{p,e} \geq 0$ and $\text{sim}_{p,e}(c, c) = 1$.*

The notion of functional code similarity can be generalized to the more discriminative functional code s -similarity.

Definition 4.3 (Functional Code s -Similarity). Consider the functional code similarity from Definition 4.1 and the

additional sharpness exponent $s \in \mathbb{N}$. Then we define the s -similarity between two implementations c_1, c_2 as

$$\text{sim}_{p,e}^s(c_1, c_2) := \text{sim}_{p,e}(c_1, c_2)^s.$$

Functional s -similarity is still a kernel for any sharpness $s \in \mathbb{N}$ and approaches functional equivalence as $s \rightarrow \infty$.

Proposition 4.4. *The functional s -similarity is a PSD kernel for $s \in \mathbb{N}$ and converges to functional equivalence as $s \rightarrow \infty$.*

Definition 4.5 (Functional Code Equivalence). Given an environment $e \in \mathcal{E}$ and a distribution over test suites $p(t)$, we define the equivalence of two implementations c_1, c_2 as

$$\text{sim}_{p,e}^\infty(c_1, c_2) := \mathbb{1}_{O(c_1, t | e) = O(c_2, t | e) \forall t \in \mathcal{V}^*: p(t) > 0}.$$

4.1. Functional Similarity Neighborhoods

Functional equivalence is the canonical structure we must impose on \mathcal{V}^* to factor out redundant representations, but functional similarity offers a smoother objective that can be used to reduce approximation error (see Section 4.4). Functional code similarity defines similarity neighborhoods:

Definition 4.6 (Fuzzy Similarity Neighborhood). For any code $c \in \mathcal{V}^*$, let \mathcal{N}_c^s be the fuzzy set representing the neighborhood of implementations functionally similar to implementation c . It is defined by the membership function $\mu_{\mathcal{N}_c}^s : \mathcal{V}^* \rightarrow [0, 1]$ where $\mu_{\mathcal{N}_c}^s(x) := \text{sim}_{p,e}^s(c, x)$.

For functional equivalence ($s \rightarrow \infty$), the sets cease to be fuzzy and become strict equivalence classes.

Proposition 4.7 (Functional Equivalence Classes). *Define $\mathcal{N}_c^\infty = \{c' \in \mathcal{V}^* : \text{sim}_{p,e}^\infty(c, c') = 1\}$. Then $\{\mathcal{N}_c^\infty : c \in \mathcal{V}^*\}$ is a set of equivalence classes partitioning \mathcal{V}^* .*

4.2. Functional Measure Smoothing

We now lift the concepts of functional similarity and equivalence to the distribution over implementations $p(c)$.

Definition 4.8 (Fuzzy Similarity Neighborhood Probability Measure). Given a distribution over implementations $p(c)$, we define the probability measure of a fuzzy similarity neighborhood \mathcal{N}_c^s as expected membership:

$$p(\mathcal{N}_c^s) := \mathbb{E}_{c' \sim p} [\mu_{\mathcal{N}_c}^s(c')] = \sum_{c' \in \mathcal{V}^*} p(c') \text{sim}_{p,e}^s(c, c').$$

This measure aggregates the probability mass of all implementations functionally similar to c , effectively smoothing the distribution over the solution space. It allows us to consider the probability of the underlying program behavior rather than focusing on specific token strings. In the limit of strict equivalence ($s \rightarrow \infty$), $p(\mathcal{N}_c^\infty)$ recovers the probability of the behavioral equivalence class containing c . However, as we discuss next, estimating strict equivalence classes suffers from high bias and high variance, whereas smoothing with finite s reduces the latter by aggregating information from functionally proximal solutions.

4.3. Monte Carlo Estimation

In practice, precisely evaluating $p(\mathcal{N}_c^s)$ or even $\text{sim}_{p,e}^s$ is prohibitively expensive due to requiring integration over \mathcal{V}^* . An effective fallback is provided by Monte Carlo estimation:

Definition 4.9 (Monte Carlo Estimators). Let $c_i \sim p(c)$ and $t_j \sim p(t)$ i.i.d. We define the Monte Carlo estimators:

$$\begin{aligned}\widehat{\text{sim}}_{p,e;m}(c_1, c_2) &:= \frac{1}{m} \sum_{j=1}^m \frac{1}{|t_j|} \sum_k \mathbb{1}_{O_k(c_1, t_j | e) = O_k(c_2, t_j | e)} \\ \widehat{\text{sim}}_{p,e;m}^s(c_1, c_2) &:= (\widehat{\text{sim}}_{p,e;m}(c_1, c_2))^s \\ \widehat{p}_{n,m}(\mathcal{N}_c^s) &:= \frac{1}{n} \sum_{i=1}^n \widehat{\text{sim}}_{p,e;m}^s(c, c_i)\end{aligned}$$

4.4. Functional Similarity vs Functional Equivalence

In this work, we study the case where p is parameterized by a neural network (e.g., an LLM). Thus, measure smoothing is desirable for three key reasons: it introduces a beneficial inductive bias that diminishes neural approximation artifacts, it reduces the Monte Carlo estimator's bias, and it improves the estimator's signal-to-noise ratio (SNR) significantly.

Environment-Dependent Inductive Bias. Similarly behaving implementations should be assigned a similar probability mass. According to Theorem 4.10, such an inductive continuity bias is achieved by measure smoothing.

Theorem 4.10 (Inductive Bias from Measure Smoothing). Let $\text{sim}_{p,e}^s(c, c') \geq 1 - \varepsilon$ for $\varepsilon \in (0, 1)$. Then

$$|p(\mathcal{N}_c^s) - p(\mathcal{N}_{c'}^s)| \leq \sqrt{2\varepsilon}.$$

Here, the sharpness exponent s determines the granularity at which two solutions are considered similar and thus tunes the strength of the environment-dependent inductive bias.

Bias Reduction. Though $\widehat{\text{sim}}_{p,e;m}^s$ is a consistent estimator of $\text{sim}_{p,e}^s$, it is biased unless $s = 1$ (Jensen's inequality).

SNR Dominance. Beyond smoothing the probability landscape, the smooth similarity estimator $\widehat{\text{sim}}_{p,e;m}^s$ is strictly superior to the sharp equivalence estimator $\widehat{\text{sim}}_{p,e;m}^1$ in SNR.

Theorem 4.11 (SNR Dominance). Let $\text{sim}_{p,e}(c_1, c_2) = \mu \in (0, 1)$ be the true functional similarity. We define the signal-to-noise Ratio (SNR) of an estimator \widehat{X} as $\text{SNR}(\widehat{X}) := (\mathbb{E}[\widehat{X}])^2 / \text{Var}(\widehat{X})$. For any number of test suites $m \geq 1$, the SNR of the smooth estimator dominates the sharp estimator by a factor of at least m^2 :

$$\frac{\text{SNR}(\widehat{\text{sim}}_{p,e;m}^s)}{\text{SNR}(\widehat{\text{sim}}_{p,e;m}^1)} \geq m(1/\mu)^{m-1} \cdot \frac{1-\mu^m}{1-\mu} \geq m^2$$

Note that Theorem 4.11 contains both a uniform lower bound of m^2 , and the much stronger μ -dependent lower bound in $\Omega(m(1/\mu)^m)$. Thus, the SNR dominance is most pronounced for small μ , i.e., given diverse code generations.

4.5. A Dual Expression for Code Correctness

Revisit the generative process of Figure 2. Given an environment $e \in \mathcal{E}$ and an executable specification $t \in \mathcal{V}^*$, the implementation $c \in \mathcal{V}^*$ is such that $R(c, t | e) = 1$. Thus, assuming a calibrated model $p(c, t)$, the following holds:

Definition 4.12 (Code-Test Calibration). A model $p(c, t)$ is code-test calibrated in an environment $e \in \mathcal{E}$ if

$$p(\mathcal{N}_c^\infty) = \mathbb{P}_{t \sim p}[R(c, t | e) = 1].$$

Hence, instead of aggregating the probability mass of equivalent codes into $p(\mathcal{N}_c^\infty)$, one may directly approximate the right-hand side expression via Monte Carlo estimation of

$$\mathbb{P}_{t \sim p}[R(c, t | e) = 1] = \mathbb{E}_{t \sim p}[R(c, t | e)^\infty] \approx \hat{\mathbb{E}}_{t_{1:m}}[R^\infty].$$

In analogy to $p(\mathcal{N}_c^1)$, the smooth estimator $\hat{\mathbb{E}}_{t_{1:m}}[R(c, t | e)]$ is also considered. As before, the SNR dominance of Theorem 4.11 still applies, motivating the smooth variant.

4.6. Maximizing Pass@k via Probability of Correctness

Thus far, we have developed robust estimators of code correctness $p(\mathcal{N}_c^\infty)$. As Proposition 4.13 demonstrates, such estimators can be immediately utilized to maximize Pass@k.

Proposition 4.13 (Additivity). Let $\text{Pass}@k(\{\mathcal{N}_{c_i}^\infty\}_{i=1}^k) := \mathbb{P}_{t \sim p}[\exists i \in \{1, \dots, k\} : R(c_i, t | e) = 1]$. Assume a code-test calibrated model $p(c, t)$ with well-specification (Assumption 4.14). Then Pass@k is maximized by greedily selecting the k code classes $\{\mathcal{N}_c^\infty\}_{1:k}$ with largest $p(\mathcal{N}_c^\infty)$.

Assumption 4.14 (Well-Specification). The test suite $t \in \mathcal{V}^*$ verifying an implementation $c \in \mathcal{V}^*$ in environment $e \in \mathcal{E}$ is almost surely such that $\exists! \mathcal{N}_c^\infty$ with $R(c, t | e) = 1$.

Proposition 4.13 justifies why $p(\mathcal{N}_c^\infty)$ is the canonical measure of solution correctness: it maximizes Pass@k.

4.7. Popular Selection Heuristics as Self-Consistency

Our framework allows us to identify several well-established selection heuristics as maximizing an estimate of the proba-

Table 1. Post-generation selection heuristics can be interpreted as adopting different estimators of $p(\mathcal{N}_c^\infty)$ to maximize Pass@k. The test output \mathbb{O} is binary \mathbb{B} (pass/fail) or arbitrary \mathbb{A} . The asterisk marks that only single-test test suites were considered (Lahiri et al., 2022; Rozière et al., 2022; Le et al., 2022; Chen et al., 2024b).

	\mathbb{O}	selection criterion
MBR-EXEC HARD (Shi et al., 2022)	\mathbb{B}	$\hat{p}_{n,m}(\mathcal{N}_c^\infty)$
MBR-EXEC SOFT (Shi et al., 2022)	\mathbb{B}	$\hat{p}_{n,m}(\mathcal{N}_c^1)$
ALPHACODE (Li et al., 2022)	\mathbb{A}	$\hat{p}_{n,m}(\mathcal{N}_c^\infty)$
FUNCODER (Chen et al., 2024a)	\mathbb{A}	$\hat{p}_{n,m}(\mathcal{N}_c^1)$
MAXPASS HARD (various work*)	\mathbb{B}	$\hat{\mathbb{E}}_{t_{1:m}}[R^\infty]$
MAXPASS SOFT (ours)	\mathbb{B}	$\hat{\mathbb{E}}_{t_{1:m}}[R]$
CODET HARD (Chen et al., 2023)	\mathbb{B}	$\hat{p}_{n,m}(\mathcal{N}_c^\infty) \hat{\mathbb{E}}_{t_{1:m}}[R]$
CODET SOFT (ours)	\mathbb{B}	$\hat{p}_{n,m}(\mathcal{N}_c^1) \hat{\mathbb{E}}_{t_{1:m}}[R]$

bility of correctness $p(\mathcal{N}_c^\infty)$. Table 1 provides a summary of the code selection literature based on our formalism. In the experimental Section 6, we focus on boolean test outputs \mathbb{O} , i.e., the canonical case of test-driven development.

MBR-EXEC Under the minimum Bayes risk decoding strategy (Shi et al., 2022), a set of codes $c_1, \dots, c_n \in \mathcal{V}^*$ and test suites $t_1, \dots, t_m \in \mathcal{V}^*$ are sampled according to the LLM posteriors $p(c)$ and $p(t)$ given a task description $d \in \mathcal{V}^*$. Then, a code $\hat{c} = \arg \min_{c_j \in c_1, \dots, c_n} \sum_{i \neq j} \ell(c_i, c_j)$ is selected to minimize an empirical estimate of the Bayes risk $\mathbb{E}_{c' \sim p}[\ell(c, c')]$ with risk function ℓ . The risk ℓ is chosen either as $-\widehat{\text{sim}}_{p,e;m}(c, c' | e)$ or $-\widehat{\text{sim}}_{p,e;m}(c, c' | e)$, resulting in MBR-EXEC HARD and MBR-EXEC SOFT, respectively.

ALPHACODE and FUNCODER Li et al. (2022) and Chen et al. (2024a) do not sample boolean-valued test cases from the language model, but rather execution scripts that invoke the code at arbitrary inputs. In our formalism, they apply generalized test suites t that return a vector of non-boolean outputs $\mathbb{A}^{|t|}$, which is then compared to estimate functional similarity. Whereas ALPHACODE relies on functional equivalence by estimating $\widehat{\text{sim}}_{p,e;m}^\infty(c, c' | e)$, FUNCODER relaxes this to functional similarity $\widehat{\text{sim}}_{p,e;m}(c, c' | e)$.

MAXPASS Proposition 4.13 hinges on a calibrated model with $p(\mathcal{N}_c^\infty) = \mathbb{P}_{t \sim p}[R(c_i, t | e) = 1]$. Instead of relying on a calibrated $p(c, t)$, one can directly estimate the right-hand side expression using $p(t)$ and a Monte Carlo estimation of $\mathbb{P}[R(c_i, t | e) = 1] = \mathbb{E}_{t \sim p}[\mathbb{1}_{R(c_i, t | e) = 1}]$. However, Monte Carlo estimators of probability of maximality have high variance (Menet et al., 2025a). To reduce the variance, one may instead consider the smooth variant $\mathbb{E}_t[R(c_i, t | e)]$. Extensive prior work by Lahiri et al. (2022); Rozière et al. (2022); Le et al. (2022); Chen et al. (2024b) investigates MAXPASS in the setting of single-test test-suites where the hard and soft estimators coincide.

CODET Chen et al. (2023) multiply the objective in the MBR-EXEC HARD strategy with the number of passed test cases. According to our formalism, they take the geometric mean of two dual estimators of self-consistency: $\hat{p}_{n,m}(\mathcal{N}_c^\infty)$ and $\hat{\mathbb{E}}_{t_{1:m}}[R(c, t | e)]$. With their method, they argue for increased robustness. Based on the insights from Section 4.4, we extend CODET with a soft variant (CODET SOFT) that adopts the smooth estimator $\hat{p}_{n,m}(\mathcal{N}_c^\infty)$. As demonstrated in the experimental section, our smooth variant of CODET performs consistently better than the original hard variant.

5. Environment Feedback during Generation

Having demonstrated the utility of the environment for post-generation selection, we now turn to feedback *during* generation.

Recall from Figure 2 that both the executable specification (test suite) and the implementation depend causally on the latent abstract algorithm $a \in \mathcal{A}$ and the execution environment $e \in \mathcal{E}$. Whereas the abstract algorithm remains unobservable beyond the task description $d \in \mathcal{V}^*$, the environment can be probed to retrieve properties like *syntax rules* and *library behaviors* via execution results $R(c, t | e) \in [0, 1]$ or descriptive reports $U(c, t | e) \in \mathcal{V}^*$.

5.1. Backprompting Approximates Thompson Sampling

To permit theoretical analysis of backprompting, we model the iterative refinement loop as a sequential bandit problem where the LLM acts as an in-context conditioned policy. We define an action $x := (c, t)$ as a pair consisting of an implementation and a test suite. Thompson sampling then selects an action x according to the probability that it is the optimal solution x^* given the task d and observation history \mathcal{H}_n , i.e., its policy is $\pi(x | \mathcal{H}_n, d) := \mathbb{P}[x = x^* | \mathcal{H}_n, d]$.

We argue that autoregressive generation, when conditioned on environment feedback, can approximate this policy. Pre-training data naturally contains description-attempt-solution triplets (d, \mathcal{H}, x^*) —for example, software repositories where commit histories document failed attempts prior to a verified solution. Following Sutter et al. (2025), training a sequence model on such trajectories with a cross-entropy loss forces the model to minimize the Kullback-Leibler divergence to the true conditional distribution of the optimum:

$$\theta^* := \operatorname{argmin}_\theta \mathbb{E}_{(d, \mathcal{H}, x^*) \sim p_{\text{data}}} [-\log p_\theta(x^* | \mathcal{H}, d)] = \operatorname{argmin}_\theta \mathbb{E}_{(d, \mathcal{H}) \sim p_{\text{data}}} [D_{KL}(p_{\text{data}}(x^* | \mathcal{H}, d) || p_\theta(x^* | \mathcal{H}, d))].$$

Hence, by backprompting failed attempts during generation, we sample $x_{n+1} \sim p_\theta(\cdot | \mathcal{H}_n, d)$, effectively sampling from the model’s learned belief over the optimal solution x^* .

This equivalence allows us to lift regret bounds from Bayesian optimization to our setting. We establish a novel regret bound for Thompson sampling which accounts for unobservable reward components, reflecting irreducible under-specification of the abstract algorithm in the task description.

5.2. A Bayesian Regret Bound for Thompson Sampling with Unobservable Reward Components

Suppose a reward function $r(x) = r_{\text{obs}}(x) + r_{\text{hid}}(x)$. For us, $r_{\text{obs}}(c, t) = R(c, t | e)$ is an observable consistency score between codes, tests, and environments. In contrast, $r_{\text{hid}}(c, t)$ may denote the task relevancy of (c, t) to the unobservable latent algorithm $a \in \mathcal{A}$, partially described by $d \in \mathcal{V}^*$.

We consider the regret against the true optimal solution $x^* := \arg \max_x r(x)$. Under Gaussian process priors for the rewards, backprompting—viewed as approximate Thompson sampling—satisfies the following regret bound:

Theorem 5.1. Define the reward $r(x) := r_{obs}(x) + r_{hid}(x)$ for $r_{obs} \sim \mathcal{N}(\mu, \Sigma)$ and $\Sigma_{x,x} \leq 1 \forall x$ as well as finite $\mathbb{E}[r_{hid}]$. Let $x_{obs}^* \sim \mathbb{P}[x^* | r_{obs}]$ and $x_n \sim \mathbb{P}[x^* | \mathcal{H}_n]$ for $x^* := \arg \max_x r(x)$ and $\mathcal{H}_n := (x_i, y_i)_{i=1}^n$. Then

$$\mathbb{E}[\sum_{n=1}^T r(x_{obs}^*) - r(x_n)] \leq \beta \sqrt{C_\sigma T \gamma_T}.$$

Here, $\gamma_T := \max_{x_{1:T}} I(r_{obs}; y_{1:T})$ is the maximum information gain for observations $y_n := r_{obs}(x_n) + \eta_n$ with independent additive noise $\eta_n \sim \mathcal{N}(0, \sigma_n^2)$ of bounded amplitude $\sigma_n \leq \sigma$. $C_\sigma = 2/\ln(1 + \sigma^{-2})$ is a small constant depending on σ , and $\beta := 1 + \sqrt{2 \log(2 \cdot |r|) + 2}$.

The regret in Theorem 5.1 is stated with respect to a Thompson sampling policy with full knowledge on r_{obs} . The regret with respect to the ground-truth optimal solution follows:

Corollary 5.2. Consider the setting of Theorem 5.1. Then for $\Delta := \mathbb{E}[r(x^*) - r(x_{obs}^*)]$ it holds that

$$\mathbb{E}[\sum_{n=1}^T r(x^*) - r(x_n)] \leq \beta \sqrt{C_\sigma T \gamma_T} + T\Delta.$$

Interpretation The bound decomposes cumulative regret into two distinct terms. The first term, $\tilde{\mathcal{O}}(\sqrt{T})$, is sub-linear and represents the *learnable* part of the problem: by interacting with the environment (running tests on implementations), the agent reduces its uncertainty about r_{obs} (syntax, library behavior, etc.). The second term, $T\Delta$, is linear. It represents the *irreducible regret*: even if the agent perfectly understands the execution environment (r_{obs}), the informal description d may still be ambiguous regarding the true latent algorithm a . No amount of execution feedback can resolve this specific ambiguity.

Remark on Gaussianity The bound assumes Gaussian rewards over finite token strings in $\mathcal{V}^{\max \text{ length}} \subseteq \mathcal{V}^*$. While finiteness is always enforced in Transformers (Vaswani et al., 2017) due to limits on the context size, Gaussianity of rewards is a stylized simplification. This assumption is standard in the analysis of Bayesian optimization (e.g., Russo & Roy 2014) and we adopt it to derive closed-form bounds that succinctly characterize the learning dynamics.

Table 2. Pass@1 (%) of the considered post-generation selection heuristics (see Table 1) after 10 rounds of independent code and test generation ($m = n = 10$). Within a family of heuristics, we bold the more accurate one. The soft variants consistently outperform the hard ones, corroborating the theoretical insights of Theorem 4.10 and Theorem 4.11. We report mean (\pm standard error) over 5 seeds.

	BigCodeBenchHard (BigCode)			QiskitHumanEvalSim (Qiskit)			LeetCodeDataset (LeetCode)		
	Qwen3	GPT-OSS	MM-M2.1	Qwen3	GPT-OSS	MM-M2.1	Qwen3	GPT-OSS	MM-M2.1
RANDOM SELECTION	27.43 ± 0.31	37.16 ± 0.63	34.46 ± 0.45	52.73 ± 0.19	41.96 ± 0.36	43.78 ± 0.47	18.60 ± 0.22	69.12 ± 0.31	62.54 ± 0.58
MBR-EXEC HARD	29.32 ± 0.43	37.30 ± 0.42	35.95 ± 0.55	54.97 ± 0.13	47.69 ± 0.40	45.73 ± 0.34	18.33 ± 0.18	72.81 ± 0.41	73.07 ± 0.33
MBR-EXEC SOFT	29.73 ± 0.42	37.30 ± 0.54	36.76 ± 0.31	54.97 ± 0.16	47.13 ± 0.35	46.71 ± 0.23	18.60 ± 0.16	72.19 ± 0.32	73.33 ± 0.45
CODET HARD	31.22 ± 0.32	37.30 ± 0.24	36.08 ± 0.59	59.02 ± 0.19	51.33 ± 0.38	50.49 ± 0.23	21.23 ± 0.12	73.25 ± 0.36	78.60 ± 0.24
CODET SOFT	35.00 ± 0.36	38.24 ± 0.34	42.03 ± 0.42	62.24 ± 0.28	54.13 ± 0.27	53.85 ± 0.33	24.30 ± 0.23	74.56 ± 0.49	79.56 ± 0.24
MAXPASS HARD	33.51 ± 0.45	37.30 ± 0.46	39.59 ± 0.39	61.40 ± 0.15	48.53 ± 0.40	51.75 ± 0.22	24.82 ± 0.26	70.09 ± 0.54	76.32 ± 0.50
MAXPASS SOFT	35.41 ± 0.38	38.24 ± 0.34	42.30 ± 0.31	63.22 ± 0.19	54.13 ± 0.27	54.13 ± 0.34	25.09 ± 0.29	74.56 ± 0.49	79.21 ± 0.30

6. Experiments

To corroborate our theory, we empirically compare the selection heuristics unified in Section 4, and analyze the empirical performance of Thompson sampling via backprompting that we introduced in Section 5. Of particular interest is the impact of the sharpness factor s and irreducible regret Δ .

6.1. Setup

Datasets We consider three challenging datasets. *BigCodeBenchHard* is the partition of the 148/1140 most difficult tasks in BigCodeBench (Zhuo et al., 2025). It adopts the format of HumanEval (Chen et al., 2021), but covers interaction with 139 external libraries. *QiskitHumanEvalSim* is a novel subset of the 143/151 QiskitHumanEval (Vishwakarma et al., 2024) questions that can be solved without access to a real-world quantum computer, democratizing the dataset. Finally, *LeetCodeDataset* consists of 228 diverse puzzle-style questions from LeetCode released after 2024-07-01 and collected by Xia et al. (2025). In contrast to the other datasets, LeetCodeDataset typically includes example input-output pairs in natural language, significantly reducing the irreducible regret Δ identified in Corollary 5.2. For additional information, see Appendix C.1.

Models We consider three frontier open-weight LLMs: Qwen3-235B-A22B-Instruct-2507 (Qwen Team, 2025), GPT-OSS-120B (OpenAI, 2025), and MiniMax-M2.1 (Minimax, 2025). Whereas the Qwen3 model responds immediately, the others are reasoning models that spend significant compute effort in generating chain-of-thought. Only MiniMax-M2.1 is an explicit coding model. More information is provided in Appendix C.2.

6.2. Post-Generation Selection Heuristics

Consider Table 2 (and its more detailed version in Figure 5 of Appendix B), reporting on the accuracy achieved through selection heuristics applied after 10 independent code and test suite generations. The accuracy improvements over

Table 3. Pass@1 (%) after 10 rounds of in-context Thompson sampling with post-generation selection applied on top. Results are reported as mean (\pm standard error) over 5 random seeds.

	BigCode	Qiskit	LeetCode
RANDOM SELECTION	27.43 ± 0.31	52.73 ± 0.19	18.60 ± 0.22
LAST SELECTION with SELF-TEST FEEDBACK	33.11 ± 0.51	56.22 ± 0.45	72.11 ± 0.08
MAXPASS SOFT	35.41 ± 0.38	63.22 ± 0.19	25.09 ± 0.29
MAXPASS SOFT with SELF-TEST FEEDBACK	36.22 ± 0.47	60.84 ± 0.36	73.42 ± 0.17

RANDOM SELECTION are highly sensitive on the post-generation selection method, with significant gains achieved by MAXPASS and CODET strategies. In particular, note that soft estimators consistently outperform hard estimators. This confirms the theoretical insights of Section 4.4: soft estimators of probability of correctness benefit from a smoothness inductive bias and from an improved SNR.

6.3. In-Context Thompson Sampling

Next, let us consider conditioning the LLM during generation on execution results from running a potential implementation c on a test suite t . Based on the development in Section 5, we provide the language model with an informative test report $U(c, t | e) \in \mathcal{V}^*$. Since test reports can become very long, direct backprompting of all information from multiple rounds quickly becomes computationally infeasible. Thus, we compress $U(c, t | e)$ into a much shorter token sequence using the LLM. We ablate on the compression technique and the factorization of $p(c, t)$ in Section 6.5. Now, examine Figure 3, where we compare three settings:

Pass@1 with ORACLE-TEST FEEDBACK First, we consider the simplified setting where the test suite t_{oracle} is given and the model only has to find a code c such that $R(c, t_{oracle} | e) = 1$. In the formalism of Theorem 5.1, this corresponds to the setting where r_{hid} is known, which according to Corollary 5.2 permits global convergence to x^* . We observe that under these circumstances, the LLM acts as a highly effective approximate Thompson sampler, finding

solutions that are much better than what can be achieved with post-selection heuristics. Indeed, in-context Thompson sampling achieves a Pass@1 of 63.78%, 72.31%, and 72.11% across BigCodeBenchHard, QiskitHumanEvalSim, and LeetCodeDataset, notably improving on the Pass@10 of unconditioned generation: 46.35%, 67.83%, 28.60%.

Estimated Pass@1 with SELF-TEST FEEDBACK Next, we let the language model generate both codes c and test suites t , but report on $R(c, t | e)$ instead of $R(c, t_{oracle} | e)$. Note that in the formalism of Theorem 5.1, the language model is asked to optimize $r = r_{obs} + r_{hid}$, but we only report on the trajectory of $r_{obs}(x_n)$. Although the LLM successfully optimizes r_{obs} on QiskitHumanEvalSim and LeetCodeDataset, it struggles to do so for BigCodeBenchHard, demonstrating that joint optimization of code and test suite proves more challenging than only optimizing code.

Pass@1 with SELF-TEST FEEDBACK Finally, we consider the most challenging setting of optimizing $R(c, t_{oracle} | e)$ with only access to $R(c, t | e)$. Recall Corollary 5.2, which predicts a small uncertainty on r_{hid} required for success, i.e., the task description must contain sufficient information on the algorithmic behavior. Whereas on LeetCodeDataset the agent recovers almost the same trajectory as if ORACLE-TEST FEEDBACK was present, the transfer on QiskitHumanEvalSim is more modest and completely missing on BigCodeBenchHard. Since the task description on LeetCodeDataset includes input-output examples, decreasing the uncertainty of r_{hid} , our theory actually predicts these findings. In Section 6.4 we open this point up further.

Combining Feedback with Post-Generation Selection Consider Table 3, which applies the MAXPASS selection heuristic on top of in-context Thompson sampling. The 10 rounds of code and test suite generations are integrated into post-generation selection as if independently generated. The Pass@1 of Thompson sampling still benefits from post-generation selection, but the improvements are less pronounced than under independent generation (no feedback).

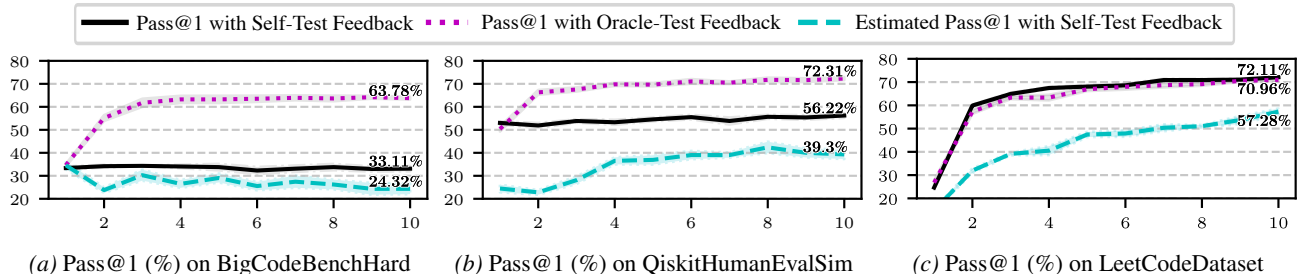


Figure 3. Pass@1 (%) during 10 rounds of in-context Thompson sampling using a Qwen3-235B-A22B-Instruct-2507. W.r.t. Theorem 5.1, the black solid line corresponds to the true reward r , and the cyan dashed line to r_{obs} . The purple dotted line is the simplified setting of known r_{hid} , which according to Corollary 5.2 permits global convergence to x^* . We report mean (\pm standard error) over 5 seeds.

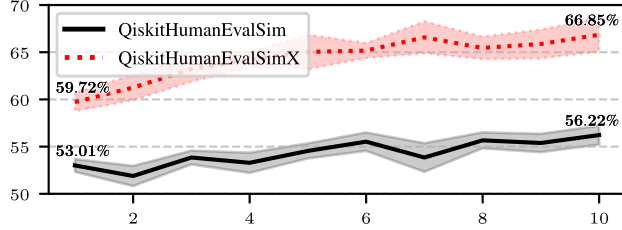


Figure 4. Pass@1 (%) during 10 rounds of in-context Thompson sampling on QiskitHumanEvalSim and QISKITHUMANEVALSIMX. We use a Qwen3-235B-A22B-Instruct-2507. Results are reported as mean (\pm standard error) over 5 random seeds.

Additional Experiments Figure 6 of Appendix B contains additional results using GPT-OSS-120B and MiniMax-M2.1 as in-context Thompson samplers. However, both perform significantly worse compared to Qwen3. In fact, neither is able to optimize SELF-TEST ACCURACY with SELF-TEST FEEDBACK, and they show diminished capabilities even when given ORACLE-TEST FEEDBACK.

6.4. QiskitHumanEvalSimX

The central lesson of Section 6.3 is that the task description d must contain sufficient information on the abstract algorithm a such that the irreducible regret Δ does not dominate the total regret of in-context Thompson sampling. An effective strategy to improve algorithmic specification is to add input-output pairs to the task description. While LeetCodeDataset already contains such behavioral examples in the prompt, explaining the success of in-context Thompson sampling thereon, BigCodeBenchHard and QiskitHumanEvalSim do not. To further corroborate our theory, we introduce a new dataset: QISKITHUMANEVALSIM WITH EXAMPLES. This new dataset builds on QiskitHumanEvalSim by querying Gemini 3 Pro to add a natural language description of the oracle test to the task description, including input-output examples if possible. The exact prompt is listed in Appendix C.1.4. As can be observed in Figure 4, in-context Thompson sampling indeed becomes more effective given the additional test description: instead of an accuracy delta over the first round of 3.21% we now report the delta 7.13%.

Table 4. Pass@1 (%) after 10 rounds of in-context Thompson sampling (with improvements during generation in parenthesis) for different factorization of $p(c, t)$ and different test report compression methods. Results reported as mean (\pm standard error) over 5 random seeds.

Compression	Factorization	BigCodeBenchHard	QiskitHumanEvalSim	LeetCodeDataset
Insights Reformulation	$p(c) \cdot p(t)$	30.81 ± 0.28 (-2.16 ± 0.32)	54.55 ± 0.33 (2.24 ± 0.33)	61.05 ± 0.32 (34.56 ± 0.48)
Insights Reformulation	$p(t c) \cdot p(c)$	31.89 ± 0.45 (-0.68 ± 0.51)	54.27 ± 0.39 (2.94 ± 0.90)	58.60 ± 0.47 (34.65 ± 0.72)
Insights Reformulation	$p(c t) \cdot p(t)$	34.05 ± 0.31 (-0.81 ± 0.46)	54.97 ± 0.19 (3.08 ± 0.40)	60.61 ± 0.48 (36.40 ± 0.30)
Summary Concatenation	$p(c) \cdot p(t)$	32.84 ± 0.45 (-0.27 ± 0.49)	55.52 ± 0.36 (3.92 ± 0.46)	71.14 ± 0.24 (42.02 ± 0.32)
Summary Concatenation	$p(t c) \cdot p(c)$	32.03 ± 0.44 (-0.41 ± 0.58)	56.08 ± 0.55 (5.45 ± 0.92)	68.42 ± 0.31 (44.74 ± 1.00)
Summary Concatenation	$p(c t) \cdot p(t)$	<u>33.11 ± 0.51</u> (-0.27 ± 0.75)	56.22 ± 0.45 (3.22 ± 0.70)	72.11 ± 0.08 (47.46 ± 0.39)

6.5. Model Factorization and Feedback Compression

In Table 4, we investigate two degrees of freedom in the implementation of in-context Thompson sampling. First, we consider different factorizations of $p(c, t)$: *independent*, *code first*, and *test first*. First generating the test suite, and then a matching implementation conditioned on the suite works best. Second, we consider different agentic compressors of test reports $U(c, t | e)$. Compression is necessary, since concatenation of the test reports themselves quickly exceeds the available memory. We ablate two compressors: iterative reformulation of past insights in light of a new test report, or concatenation of summaries of each test report. A detailed description of each is provided in Appendix C.4. We remark that *summary concatenation* outperforms *insight reformulation*, at the cost of additional memory and compute. Unless otherwise mentioned, we always report on *summary concatenation* with the factorization $p(c | t) \cdot p(t)$.

7. Conclusion

In this work, we provide a probabilistic framework for coding agents that interact with an execution environment. We theoretically formalize two dominant paradigms: post-generation selection as environment-aware Pass@k maximization, and iterative backprompting as in-context Thompson sampling. Our analysis proves that “soft” estimators strictly dominate “hard” ones in terms of SNR. Moreover, we identify an “irreducible regret” in the regret bound of Thompson sampling, where task ambiguity limits performance regardless of feedback quality. These theoretical insights are confirmed experimentally across three diverse benchmarks using three different frontier open-weight large language models. Finally, a novel benchmark, QISKITHUMANEVALSIMX, is introduced to further corroborate our findings. As LLMs are increasingly integrated into critical software development loops, understanding the theoretical mechanisms of their environment interactions is paramount. Our results suggest that future progress lies not just in improving zero-shot model performance, but also in reducing the ambiguity of user intent and designing architectures that can efficiently process long execution histories.

Impact Statement

This paper presents work whose goal is to advance the field of Machine Learning. There are many potential societal consequences of our work, none which we feel must be specifically highlighted here.

Acknowledgment

This work is supported by the Swiss National Science foundation (SNF), grant 10002666.

References

Beck, K. L. *Test-driven development - by example*. The Addison-Wesley signature series. Addison-Wesley, 2003.

Bunel, R., Hausknecht, M. J., Devlin, J., Singh, R., and Kohli, P. Leveraging grammar and reinforcement learning for neural program synthesis. In *The 6th International Conference on Learning Representations*, 2018.

Chen, B., Zhang, F., Nguyen, A., Zan, D., Lin, Z., Lou, J., and Chen, W. CodeT: Code generation with generated tests. In *The 11th International Conference on Learning Representations*, 2023.

Chen, J., Tang, H., Chu, Z., Chen, Q., Wang, Z., Liu, M., and Qin, B. Divide-and-conquer meets consensus: Unleashing the power of functions in code generation. In *Advances in Neural Information Processing Systems*, volume 37, pp. 67061–67105. Curran Associates, Inc., 2024a. doi: 10.5220/079017-2141.

Chen, M., Tworek, J., Jun, H., Yuan, Q., de Oliveira Pinto, H. P., Kaplan, J., Edwards, H., Burda, Y., Joseph, N., Brockman, G., Ray, A., Puri, R., Krueger, G., Petrov, M., Khlaaf, H., Sastry, G., Mishkin, P., Chan, B., Gray, S., Ryder, N., Pavlov, M., Power, A., Kaiser, L., Bavarian, M., Winter, C., Tillet, P., Such, F. P., Cummings, D., Plappert, M., Chantzis, F., Barnes, E., Herbert-Voss, A., Guss, W. H., Nichol, A., Paino, A., Tezak, N., Tang, J., Babuschkin, I., Balaji, S., Jain, S., Saunders, W., Hesse, C., Carr, A. N., Leike, J., Achiam, J., Misra, V., Morikawa, E., Radford, A., Knight, M., Brundage, M., Murati, M., Mayer, K., Welinder, P., McGrew, B., Amodei, D., McCandlish, S., Sutskever, I., and Zaremba, W. Evaluating large language models trained on code. *CoRR*, abs/2107.03374, 2021. doi: 10.48550/arxiv.2107.03374.

Chen, M., Liu, Z., Tao, H., Hong, Y., Lo, D., Xia, X., and Sun, J. B4: Towards optimal assessment of plausible code solutions with plausible tests. In *Proceedings of the 39th IEEE/ACM International Conference on Automated Software Engineering*, pp. 1693–1705. ACM, 2024b. doi: 10.1145/3691620.3695536.

Chen, X., Lin, M., Schärli, N., and Zhou, D. Teaching large language models to Self-Debug. In *The 12th International Conference on Learning Representations*, 2024c.

Chlon, L., Rashidi, S., Khamis, Z., and Awada, M. M. LLMs are Bayesian, in expectation, not in realization. *CoRR*, abs/2507.11768, 2025. doi: 10.48550/arxiv.2507.11768.

Lahiri, S. K., Naik, A., Sakkas, G., Choudhury, P., von Veh, C., Musuvathi, M., Inala, J. P., Wang, C., and Gao, J. Interactive code generation via test-driven user-intent formalization. *CoRR*, abs/2208.05950, 2022. doi: 10.48550/arxiv.2208.05950.

Le, H., Wang, Y., Gotmare, A. D., Savarese, S., and Hoi, S. C. CodeRL: Mastering code generation through pre-trained models and deep reinforcement learning. In *Advances in Neural Information Processing Systems*, volume 35, pp. 21314–21328. Curran Associates, Inc., 2022.

Li, Y., Choi, D. H., Chung, J., Kushman, N., Schrittweiser, J., Leblond, R., Eccles, T., Keeling, J., Gimeno, F., Lago, A. D., Hubert, T., Choy, P., de Masson d'Autume, C., Babuschkin, I., Chen, X., Huang, P., Welbl, J., Gowal, S., Cherepanov, A., Molloy, J., Mankowitz, D. J., Robson, E. S., Kohli, P., de Freitas, N., Kavukcuoglu, K., and Vinyals, O. Competition-level code generation with AlphaCode. *Science*, 378(6624):1092–1097, 2022. doi: 10.1126/science.abq1158.

Menet, N., Hübotter, J., Kassraie, P., and Krause, A. LITE: Efficiently estimating Gaussian probability of maximality. In *International Conference on Artificial Intelligence and Statistics*, volume 258 of *Proceedings of Machine Learning Research*, pp. 4996–5004. Proceedings of Machine Learning Research, 2025a.

Menet, N., Terzic, A., Hersche, M., Krause, A., and Rahimi, A. Thompson sampling via fine-tuning of LLMs. *CoRR*, abs/2510.13328, 2025b. doi: 10.48550/arxiv.2510.13328.

MiniMax. MiniMax-M1: Scaling test-time compute efficiently with lightning attention. *CoRR*, abs/2506.13585, 2025. doi: 10.48550/arxiv.2506.13585.

Olausson, T. X., Inala, J. P., Wang, C., Gao, J., and Solar-Lezama, A. Is Self-Repair a silver bullet for code generation? In *The 12th International Conference on Learning Representations*, 2024.

OpenAI. GPT-4 technical report. *CoRR*, abs/2303.08774, 2023. doi: 10.48550/arxiv.2303.08774.

OpenAI. GPT-OSS-120b & GPT-OSS-20b model card. *CoRR*, abs/2508.10925, 2025. doi: 10.48550/arxiv.2508.10925.

Qwen Team. Qwen3 technical report. *CoRR*, abs/2505.09388, 2025. doi: 10.48550/arxiv.2505.09388.

Rozière, B., Zhang, J., Charton, F., Harman, M., Synnaeve, G., and Lample, G. Leveraging automated unit tests for unsupervised code translation. In *The 10th International Conference on Learning Representations*, 2022.

Russo, D. and Roy, B. V. Learning to optimize via posterior sampling. *Mathematics of Operations Research*, 39(4): 1221–1243, 2014. doi: 10.1287/moor.2014.0650.

Shazeer, N., Mirhoseini, A., Maziarz, K., Davis, A., Le, Q. V., Hinton, G. E., and Dean, J. Outrageously large neural networks: The sparsely-gated mixture-of-experts layer. In *The 5th International Conference on Learning Representations*, 2017.

Shi, F., Fried, D., Ghazvininejad, M., Zettlemoyer, L., and Wang, S. I. Natural language to code translation with execution. In *Proceedings of the 2022 Conference on Empirical Methods in Natural Language Processing*, pp. 3533–3546. Association for Computational Linguistics, 2022. doi: 10.18653/V1/2022.EMNLP-MAIN.231.

Shinn, N., Cassano, F., Gopinath, A., Narasimhan, K., and Yao, S. Reflexion: Language agents with verbal reinforcement learning. In *Advances in Neural Information Processing Systems*, volume 36, pp. 8634–8652. Curran Associates, Inc., 2023.

Srinivas, N., Krause, A., Kakade, S. M., and Seeger, M. W. Gaussian process optimization in the bandit setting: No regret and experimental design. In *Proceedings of the 27th International Conference on Machine Learning*, pp. 1015–1022. Omnipress, 2010.

Sutter, G., Abdulrahman, M., Wang, H., Subramanian, S. G., St-Aubin, M., O’Sullivan, S., Wan, L., Ricardez-Sandoval, L. A., Poupart, P., and Kristiadi, A. Simplifying Bayesian optimization via in-context direct optimum sampling. *CoRR*, abs/2505.23913, 2025. doi: 10.48550/arxiv.2505.23913.

Thompson, W. R. On the likelihood that one unknown probability exceeds another in view of the evidence of two samples. *Biometrika*, 25(3/4):285–294, 1933. doi: 10.2307/2332286.

Vaswani, A., Shazeer, N., Parmar, N., Uszkoreit, J., Jones, L., Gomez, A. N., Kaiser, L. u., and Polosukhin, I. Attention is all you need. In *Advances in Neural Information Processing Systems*, volume 30. Curran Associates, Inc., 2017.

Vishwakarma, S., Harkins, F., Golecha, S., Bajpe, V. S., Dupuis, N., Buratti, L., Kremer, D., Faro, I., Puri, R., and Cruz-Benito, J. Qiskit HumanEval: An evaluation benchmark for quantum code generative models. In *IEEE International Conference on Quantum Computing and Engineering*, pp. 1169–1176. IEEE, 2024. doi: 10.1109/QCE60285.2024.00137.

Wang, X., Wei, J., Schuurmans, D., Le, Q. V., Chi, E. H., Narang, S., Chowdhery, A., and Zhou, D. Self-consistency improves chain of thought reasoning in language models. In *The 11th International Conference on Learning Representations*, 2023.

Wei, J., Wang, X., Schuurmans, D., Bosma, M., Ichter, B., Xia, F., Chi, E. H., Le, Q. V., and Zhou, D. Chain-of-thought prompting elicits reasoning in large language models. In *Advances in Neural Information Processing Systems*, volume 35, pp. 24824–24837. Curran Associates, Inc., 2022.

Xia, Y., Shen, W., Wang, Y., Liu, J. K., Sun, H., Wu, S., Hu, J., and Xu, X. LeetCodeDataset: A temporal dataset for robust evaluation and efficient training of code LLMs. *CoRR*, abs/2504.14655, 2025. doi: 10.48550/arxiv.2504.14655.

Xie, S. M., Raghunathan, A., Liang, P., and Ma, T. An explanation of in-context learning as implicit Bayesian inference. In *The 11th International Conference on Learning Representations*, 2022.

Zhong, Z., Guo, J., Yang, W., Peng, J., Xie, T., Lou, J., Liu, T., and Zhang, D. SemRegex: A semantics-based approach for generating regular expressions from natural language specifications. In *Proceedings of the 2018 Conference on Empirical Methods in Natural Language Processing*, pp. 1608–1618. Association for Computational Linguistics, 2018. doi: 10.18653/V1/D18-1189.

Zhuo, T. Y., Vu, M. C., Chim, J., Hu, H., Yu, W., Widyasari, R., Yusuf, I. N. B., Zhan, H., He, J., Paul, I., Brunner, S., Gong, C., Hoang, T., Zebaze, A. R., Hong, X., Li, W.-D., Kaddour, J., Xu, M., Zhang, Z., Yadav, P., Jain, N., Gu, A., Cheng, Z., Liu, J., Liu, Q., Wang, Z., Hui, B., Muennighoff, N., Lo, D., Fried, D., Du, X., de Vries, H., and Werra, L. V. BigCodeBench: Benchmarking code generation with diverse function calls and complex instructions. In *The 13th International Conference on Learning Representations*, 2025.

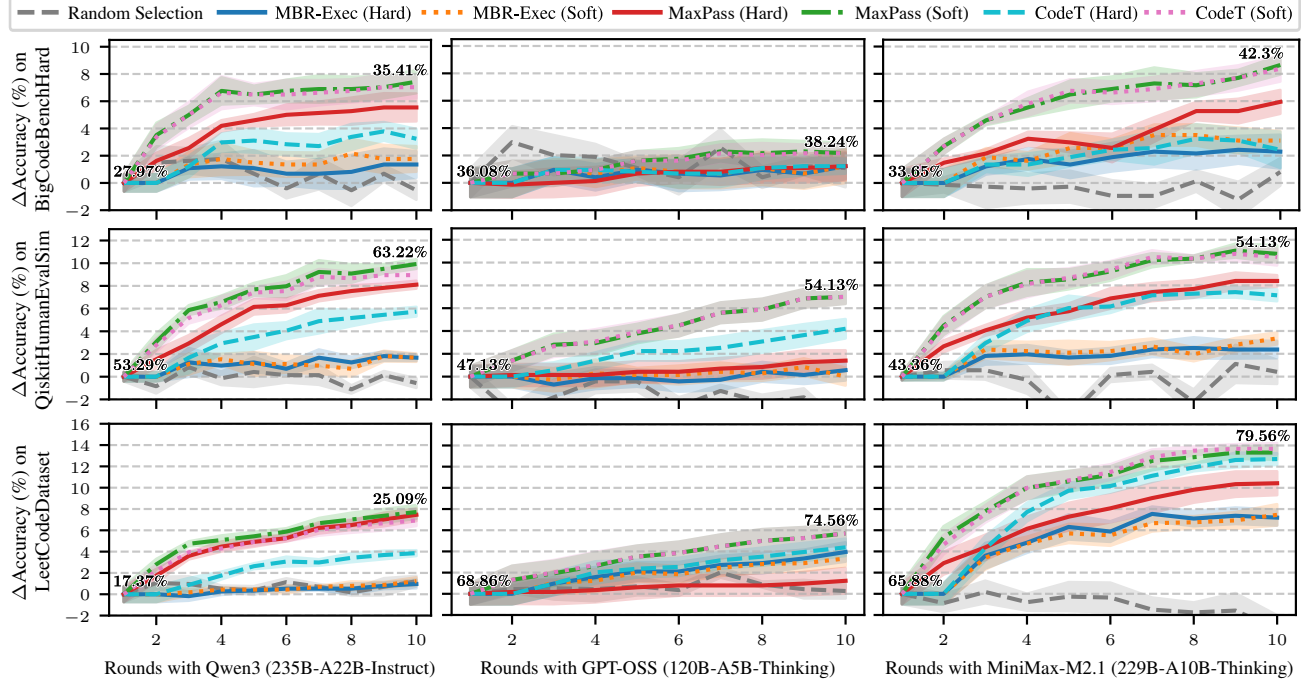


Figure 5. Pass@1 (%) improvements of common post-generation selection heuristics (see Table 1 and Table 2) across BigCodeBenchHard, QiskitHumanEvalSim, and LeetCodeDataset. Qwen3-235B-A22B-Instruct-2507, GPT-OSS-120B, or MiniMax-M2.1 are used to independently generate code and tests across multiple rounds. Results are reported as mean (\pm standard error) over 5 random seeds.

A. Discussion

Computational Cost of Environment-Aware Selection Our theoretical analysis confirms that the environment-aware selection heuristics in Table 1 approximately maximize the probability of correctness. Unfortunately, selection comes at a non-negligible computational cost. Specifically, heuristics such as MBR-EXEC, CODET, and MAXPASS require cross-executing n generated implementations against m generated test suites. This results in a quadratic scaling of compute cost, $\mathcal{O}(n \times m)$. While this is manageable for the lightweight tasks considered in our experiments and the small budget of 10 rounds, it can introduce a significant bottleneck for large-scale software engineering tasks where compiling and running integration tests can be time-consuming. In fact, even on QiskitHumanEvalSimX with a single node using an AMD EPYC 7763 64-Core CPU, 2TB RAM, and 8 NVIDIA A100-SXM4 GPUs (80GB), the costs are non-negligible. Whereas 10 rounds of in-context Thompson sampling across 5 seeds (with test-first factorization and *summary concatenation* using a Qwen3-235B-A22B-Instruct-2507) take 12 hours and 42 minutes, running all implementations on all test suites for post-generation selection already dominates at 21 hours and 32 minutes.

Contextual Overhead in Iterative Backprompting Beyond execution cost, iterative refinement via backprompting introduces significant context overhead. As detailed in Section 5, effective in-context Thompson sampling relies on providing the model with historical feedback. Our *summary concatenation* approach, while effective, linearly increases the prompt length with every interaction round. Given the quadratic complexity of the attention mechanism in Transformer architectures, this limits the number of feasible iterations. Indeed, 10 rounds of in-context Thompson sampling across 5 seeds (with test-first factorization and *summary concatenation* using a Qwen3-235B-A22B-Instruct-2507) processes 118 865 154 total tokens of which only 16 964 129 are newly generated. Model architectures with linear complexity, such as State-Space Models (SSMs) or Linear Transformers, may be better suited for agents engaging in prolonged environment interactions, allowing them to dynamically compress or retain feedback history without prohibitive compute costs.

The Critical Role of Test Synthesis Capabilities Our framework posits that the utility of the environment is bounded by the quality of the executable specification t . This dependency explains the counter-intuitive performance of GPT-OSS-120B. Despite possessing strong one-shot code generation capabilities comparable to other frontier models, GPT-OSS failed to benefit significantly from environment interaction strategies (see Figure 6). Qualitatively, we observed that

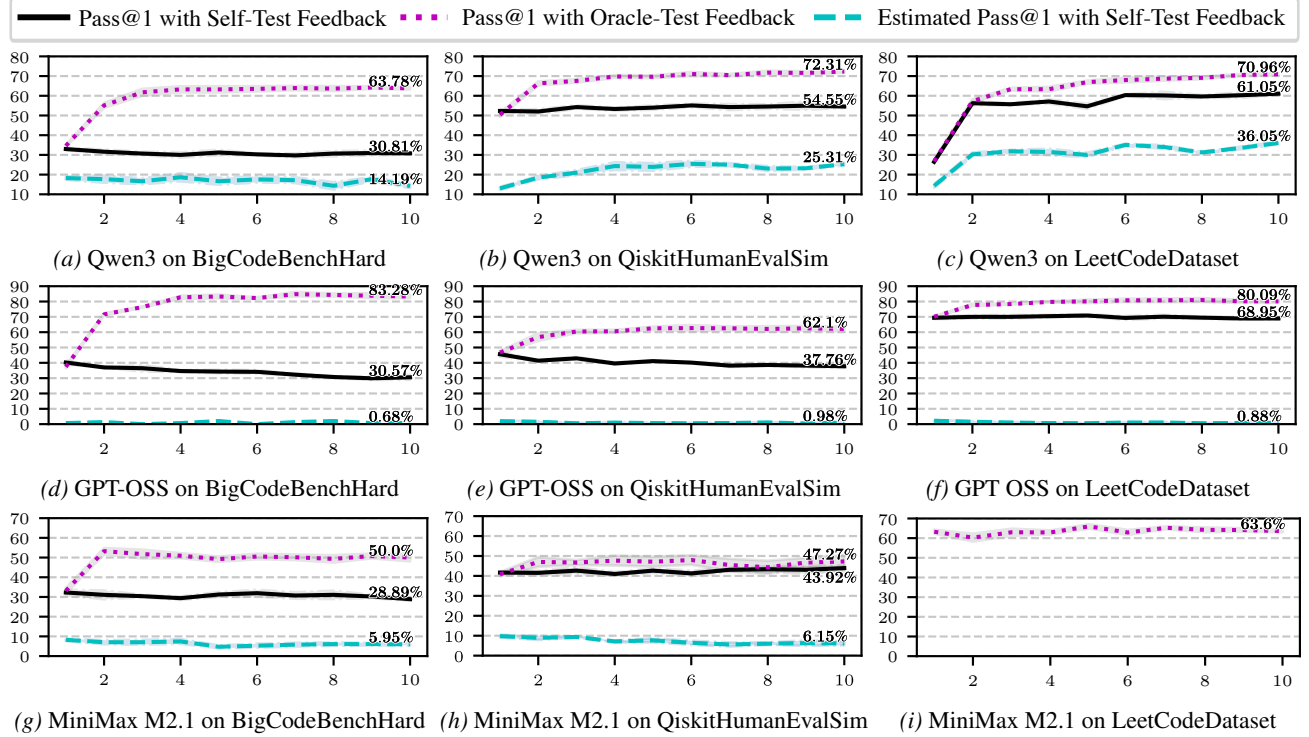


Figure 6. Pass@1 (%) of in-context Thompson sampling via backprompting with Qwen3-235B-A22B-Instruct-2507, GPT-OSS-120B, and MiniMax-M2.1 across BigCodeBenchHard, QiskitHumanEvalSim, and LeetCodeDataset. In the language of Theorem 5.1, the black solid line corresponds to the true reward r , and the cyan dashed line to r_{obs} . The purple dotted line corresponds to the case of known r_{hid} , which according to Corollary 5.2 permits global convergence to x^* . Results are reported as mean (\pm standard error) over 5 random seeds.

GPT-OSS frequently generates invalid tests. Without the ability to synthesize high-quality, discriminative tests, the signal $R(c, t | e)$ becomes noisy, rendering both post-generation selection and backprompting less effective. This highlights that for autonomous software engineering, the ability to verify code (via test writing) is just as critical as the ability to write code.

B. Additional Experiments

Selection after Generation We complement Table 2 with Figure 5, which details the accuracy improvements achieved after generation through the considered selection heuristics. We plot the improvement as a function of the number of rounds of code and test suite generations. In several settings the accuracy improvements do not yet saturate after 10 rounds, but the compute cost of post-generation selection starts to dominate the generation cost using a Qwen3-235B-A22B-Instruct, even for massive parallelism with 64 CPU cores (AMD EPYC 7763) for selection and only a single node with 8 GPUs (NVIDIA A100 80GB) for generation. See Appendix A for runtime measurements. This runtime bottleneck stems from the quadratic scaling of post-generation selection, as every code must be executed on every test suite.

Feedback during Generation With Figure 6, we extend Figure 3 to include results on GPT-OSS-120B and MiniMax-M2.1 in addition to Qwen3-235B-A22B-Instruct. Whereas Figure 3 reports on *summary concatenation* and *test-first* factorization ($p(c, t) = p(c|t) \cdot (t)$), Figure 6 adopts *insight reformulation* and *independent* factorization ($p(c, t) = p(c) \cdot (t)$) throughout. Note that Qwen3-235B-A22B-Instruct is a more effective approximate Thompson sampler. Indeed, given ORACLE-TEST FEEDBACK (purple dotted line), Qwen3-235B-A22B-Instruct demonstrates significantly stronger accuracy improvements than MiniMax-M2.1, whose gains saturate after just one round. Moreover, both GPT-OSS-120B and MiniMax-M2.1 generate test suites that are much worse. In fact, given SELF-TEST FEEDBACK, the SELF-TEST ACCURACY (cyan dashed line) is much lower than the actual ORACLE-TEST ACCURACY (black solid line). As a result, these two model receive highly noisy environment feedback and therefore no accuracy gains over the zero-shot performance can be achieved.

C. Experimental Details

To ensure reproducibility, we complement Section 6 with a more detailed description of the experimental setup. All experiments were conducted on compute nodes with an AMD EPYC 7763 64-Core CPU, 2TB RAM, and eight NVIDIA A100-SXM4 GPUs (80GB), running on Red Hat Enterprise Linux 9.4 with CUDA 12.4. Our code is provided in the supplementary materials, including experimental configuration files and environment files specifying the necessary Python packages and their versions, and will be released publicly under a permissive license upon acceptance.

C.1. Datasets

C.1.1. BIGCODEBENCHHARD

The partition of the 148/1140 most challenging tasks in BigCodeBench (Zhuo et al., 2025). BigCodeBench is designed for function-level code generation, adopting the format of HumanEval (Chen et al., 2021). The tasks in BigCodeBench require multiple external libraries across 7 domains including networking, data analysis, and visualization. The benchmark tests compositional reasoning and the ability to implement complex instructions that span 139 libraries with an average of 2.8 libraries per task.

C.1.2. QISKITHUMANEVALSIM

A novel subset of QiskitHumanEval (Vishwakarma et al., 2024) that we introduce. It consists of the subset of the 143/151 questions (excluding task ids 43, 97, 98, 122, 129, 133, 134, 146 of which 6 are classified as basic, 2 as intermediate, and none as difficult) that can be solved without access to a real-world quantum computer (i.e., simulated), democratizing the dataset. Due to the small fraction of training data being dedicated to Qiskit during typical LLM training, and since Qiskit’s API has undergone multiple backward-incompatible changes, QiskitHumanEvalSim is a great testbed for agentic environment interaction.

C.1.3. LEETCODEDATASET v0.3.1

228 diverse puzzle-style questions from LeetCode released after 2024-07-01 and collected by Xia et al. (2025). LeetCode typically includes example input-output pairs in natural language, significantly reducing the irreducible regret Δ identified in Corollary 5.2 and, as we show, enabling more effective in-context Thompson sampling.

C.1.4. QISKITHUMANEVALSIMX

QISKITHUMANEVALSIMX is a novel benchmark that we introduce in order to corroborate our theory, in particular the insight that effective in-context Thompson sampling requires a task description $d \in \mathcal{V}^*$ with small uncertainty on the latent algorithm $a \in \mathcal{A}$ (see Theorem 5.1 and its Corollary 5.2). We improve the specification of the algorithm in d by describing its target behavior in more detail, including input-output examples. More precisely, to create QISKITHUMANEVALSIMX from QiskitHumanEvalSim, we query Google Gemini 3 Pro (January 10, 2026) using the following prompt template:

Consider the following dataset entry:

```
```
{"task_id": "qiskitHumanEval/35", "prompt": "from qiskit.circuit.library [...]
```

```

Improve the docstring in the prompt by appending a natural language description of the test without leaking the canonical solution. The natural language description must be detailed, but must not contain code. If the test contains an input-output example, provide it. Don’t explicitly mention the presence of tests. Don’t change anything else. Return the improved dataset entry in the jsonl format.

In case the instructions were not followed or invalid symbols were returned, the query was repeated. The resulting dataset was verified by running all canonical solutions against the oracle test suite.

C.2. Models

We consider three frontier open-weight LLMs, with an emphasis on qualitative differences such as reasoning vs instruct and general-purpose vs coding. We sample directly from the model with temperature 1.0 and top-p set to 0.95. After exceeding 32 768 output tokens generation is stopped. In case invalid output is generated (e.g., if no code or observations can be extracted) we repeat up to 9 times the same query to the LLM. The investigated models are as follows:

Qwen3-235B-A22B-Instruct-2507 is the largest publicly available instruction-tuned model in the general-purpose Qwen3 model family (Qwen Team, 2025). Adopting the mixture of experts (MoE) architecture (Shazeer et al., 2017), only 22 out of the 235 billion parameters are active at inference. The model is **not trained for chain-of-thought** (Wei et al., 2022).

GPT-OSS-120B is the largest publicly available model released by OpenAI (OpenAI, 2025). It is a general-purpose reasoning model trained for long **chain-of-thoughts**. Tallying a total of 120 billion parameters, but with only 5B active, it is optimized for high throughput.

MiniMax-M2.1 is a novel state-of-the-art **coding** model released on the 23rd of December 2025, building on the MiniMax-M1 architecture (MiniMax, 2025). It is an MoE with 229 billion total parameters, of which only 10B are active. It is trained for and **utilizes chain-of-thought** for reasoning.

C.3. Implementation-Test Suite Generation Prompts

In the following, we list the system prompts used for implementation and test suite generation, adopting the factorization $p(c, t) = p(c | t)p(t)$. The prompts for the alternative factorizations are adjusted accordingly and listed in the code base.

Test Suite Generation

You are an expert Python programmer.

Your task is to write pytests for an implementation that obeys the provided task description. You are provided observations from previous rounds of comparing potential implementations against potential test suites.

1. Analyze and Plan

- Carefully reflect on the provided observations.
- Your new test suite must address these observations while still covering the program's main functionality and common edge cases.

2. Write the test suite

- Include all necessary imports for external libraries. The candidate implementation is available without imports.
- Each pytest must be represented by a separate function starting with 'test_'. In particular, do not define test classes.
- Add a brief docstring to each pytest function explaining its purpose.
- Do not number the pytests.
- Provide all of the pytests in a single Python code block marked with triple backticks (```).

Implementation Generation

You are an expert Python programmer.

Your task is to write an implementation that obeys the provided task description. You are provided observations from previous rounds of comparing potential implementations against potential test suites, as well as a novel test suite.

1. Analyze and Plan

- Carefully reflect on the provided observations.
- Review the provided test suite.

- Your new implementation must address the observations, pass all test cases, and adhere to the original task description.

****2. Write the implementation****

- Include all necessary imports for external libraries.
- Do not include a docstring.
- Write the program in a Python code block marked with triple backticks (```).

C.4. Feedback Compressor

We consider two strategies for compression of the test reports. With *insight reformulation*, we not only compress each report into actionable insights, but also reformulate old insights to avoid insight duplication and to ensure the context size only increases if new information is acquired. In contrast, with *summary concatenation*, we simply ask the LLM to compress the test report of each round into a summary, which are then concatenated in the prompt. This ensures no information is accidentally lost, but results in a context that grows linearly with the number of rounds of in-context Thompson sampling.

Insight Reformulation

You are an expert Python programmer.

You are provided a task description, a candidate program implementation, a candidate test suite with feedback on the implementation, and additional past observations.

Your task is to first analyze the test feedback and then state an exhaustive list of insights that acts as a compressed history of all observations.

****1. Analyze Feedback****

- Carefully review the program, tests, and feedback. This is your new data.
- Identify errors in the program implementation, as well as weaknesses in the tests themselves.
- Summarize all your findings. Be precise and do not speculate.

****2. State Insights****

- Restate all insights from past observations as well as additional insights from the feedback analysis.
- Mark each insight with '<observation> </observation>' tags.
- Ensure each insight is self-contained, i.e., informative without considering the provided program and test suite.

Summary Concatenation

You are an expert Python programmer.

You are provided a task description, a candidate program implementation, and a candidate test suite with feedback on the implementation.

Your task is to first analyze the test feedback and then summarize the implementation, tests, and feedback.

****1. Analyze Feedback****

- Carefully review the program, tests, and feedback. This is your data.
- Identify errors in the program implementation, as well as weaknesses in the tests themselves.

****2. State Summary****

- Summarize the provided implementation, test suite, and all your findings.
- Mark the summary with '<observation> </observation>' tags.

D. Proofs

Proposition 4.2. *The similarity $\text{sim}_{p,e}(c_1, c_2)$ is a positive semi-definite (PSD) kernel with $\text{sim}_{p,e} \geq 0$ and $\text{sim}_{p,e}(c, c) = 1$.*

Proof. We first show that $\text{sim}_{p,e}$ is a positive semi-definite (PSD) kernel. Recall Definition 4.1:

$$\text{sim}_{p,e}(c_1, c_2) := \mathbb{E}_{t \sim p} \left[\frac{1}{|t|} \sum_{k=1}^{|t|} \mathbb{1}_{O_k(c_1, t|e) = O_k(c_2, t|e)} \right]$$

Let \mathbb{O} be the set of possible test outputs, i.e., $O_k(c, t|e) \in \mathbb{O} \forall c, t, k$ under the specified environment $e \in \mathcal{E}$. For a fixed test t and index k , define the feature map $\phi_{t,k} : \mathcal{V}^* \rightarrow \{0, 1\}^{|\mathbb{O}|}$ such that $\phi_{t,k}(c)$ is a one-hot vector corresponding to the output $O_k(c, t|e)$. The indicator function can then be written as an inner product:

$$\mathbb{1}_{O_k(c_1, t|e) = O_k(c_2, t|e)} = \langle \phi_{t,k}(c_1), \phi_{t,k}(c_2) \rangle.$$

Since the inner product is a valid kernel, and the class of kernels is closed under addition and scaling by non-negative constants (linearity of expectation), $\text{sim}_{p,e}(c_1, c_2)$ is a valid kernel. Concerning non-negativity: The indicator function is non-negative, and the probability measure $p(t)$ is non-negative, thus $\text{sim}_{p,e}(c_1, c_2) \geq 0$. Finally, the kernel is normalized since

$$\text{sim}_{p,e}(c, c) = \mathbb{E}_{t \sim p} \left[\frac{1}{|t|} \sum_{k=1}^{|t|} \mathbb{1}_{O_k(c, t|e) = O_k(c, t|e)} \right] = \mathbb{E}_{t \sim p} [1] = 1. \quad \square$$

Proposition 4.4. *The functional s -similarity is a PSD kernel for $s \in \mathbb{N}$ and converges to functional equivalence as $s \rightarrow \infty$.*

Proof. From Proposition 4.2, we established that the base similarity $\text{sim}_{p,e}(c_1, c_2)$ is a kernel. The class of positive semi-definite kernels is closed under point-wise multiplication (as a consequence of the Schur Product Theorem). Since $\text{sim}_{p,e}^s(c_1, c_2) = \text{sim}_{p,e}(c_1, c_2)^s$ is the point-wise product of the kernel $\text{sim}_{p,e}$ with itself s times, $\text{sim}_{p,e}^s$ is a kernel for any $s \in \mathbb{N}$. To prove convergence to functional equivalence, consider two cases: If $\text{sim}_{p,e}^\infty(c_1, c_2) = 1$ then $O_k(c_1, t|e) = O_k(c_2, t|e) \forall k \in [|t|], t \in \mathcal{V}^* : p(t) > 0$. Therefore, $\text{sim}_{p,e}(c, c) = 1$ and thus $\text{sim}_{p,e}^s(c, c) = 1 \forall s \in \mathbb{N}$, including in the limit. In contrast, if $\text{sim}_{p,e}^\infty(c_1, c_2) \neq 1$, then $\text{sim}_{p,e}^\infty(c_1, c_2) = 0$ and $\exists k \in [|t|], t \in \mathcal{V}^* : p(t) > 0$ and $O_k(c_1, t|e) \neq O_k(c_2, t|e)$. But then $\text{sim}_{p,e}(c_1, c_2) \in [0, 1)$ and thus $\lim_{s \rightarrow \infty} \text{sim}_{p,e}^s(c_1, c_2) = \lim_{s \rightarrow \infty} \text{sim}_{p,e}(c_1, c_2)^s = 0$. In either case, functional s -similarity converges to functional equivalence as $s \rightarrow \infty$. \square

Proposition 4.7. *Define $\mathcal{N}_c^\infty = \{c' \in \mathcal{V}^* : \text{sim}_{p,e}^\infty(c, c') = 1\}$. Then $\{\mathcal{N}_c^\infty : c \in \mathcal{V}^*\}$ is a set of equivalence classes partitioning \mathcal{V}^* .*

Proof. By Definition 4.5, $\text{sim}_{p,e}^\infty(c, c') = 1$ if and only if the codes c, c' produce identical outputs on all test cases with non-zero support. Since the equality of outputs is reflexive, symmetric, and transitive, $\text{sim}_{p,e}^\infty$ inherits these properties, partitioning the code space into disjoint equivalence classes \mathcal{N}_c^∞ . \square

Theorem 4.10. *Let $\text{sim}_{p,e}^s(c, c') \geq 1 - \varepsilon$ for $\varepsilon \in (0, 1)$. Then*

$$|p(\mathcal{N}_c^s) - p(\mathcal{N}_{c'}^s)| \leq \sqrt{2\varepsilon}.$$

Proof. Since $\text{sim}_{p,e}^s$ is a positive definite kernel with $\text{sim}_{p,e}^s(c, c) = 1$ (from Proposition 4.2), there exists a feature map $\phi : \mathcal{V}^* \rightarrow \mathcal{H}$ into a Hilbert space such that $\text{sim}_{p,e}^s(x, y) = \langle \phi(x), \phi(y) \rangle$ and $\|\phi(x)\| = 1$.

We can express the probability of the fuzzy neighborhood $p(\mathcal{N}_c^s)$ as an inner product with the *mean embedding* of the distribution p . Let $\mu_p := \mathbb{E}_{x \sim p}[\phi(x)]$. Then:

$$\begin{aligned} p(\mathcal{N}_c^s) &= \mathbb{E}_{x \sim p}[\text{sim}_{p,e}^s(c, x)] \\ &= \mathbb{E}_{x \sim p}[\langle \phi(c), \phi(x) \rangle] = \langle \phi(c), \mu_p \rangle. \end{aligned}$$

The difference in probability mass is then governed by the distance in feature space:

$$\begin{aligned} |p(\mathcal{N}_c^s) - p(\mathcal{N}_{c'}^s)| &= |\langle \phi(c), \mu_p \rangle - \langle \phi(c'), \mu_p \rangle| \\ &= |\langle \phi(c) - \phi(c'), \mu_p \rangle|. \end{aligned}$$

Applying the Cauchy-Schwarz inequality yields:

$$|\langle \phi(c) - \phi(c'), \mu_p \rangle| \leq \|\phi(c) - \phi(c')\| \cdot \|\mu_p\|.$$

We bound the first term using the similarity condition:

$$\begin{aligned} \|\phi(c) - \phi(c')\|^2 &= \langle \phi(c) - \phi(c'), \phi(c) - \phi(c') \rangle \\ &= \|\phi(c)\|^2 + \|\phi(c')\|^2 - 2\langle \phi(c), \phi(c') \rangle \\ &= 2 - 2\text{sim}_{p,e}^s(c, c') \leq 2 - 2(1 - \varepsilon) = 2\varepsilon. \end{aligned}$$

Thus, $\|\phi(c) - \phi(c')\| \leq \sqrt{2\varepsilon}$. For the second term, by Jensen's inequality, the norm of the mean embedding is bounded by the expected norm:

$$\|\mu_p\| = \|\mathbb{E}_x[\phi(x)]\| \leq \mathbb{E}_x[\|\phi(x)\|] = 1.$$

Multiplying these bounds gives $|p(\mathcal{N}_c^s) - p(\mathcal{N}_{c'}^s)| \leq \sqrt{2\varepsilon} \cdot 1$. \square

Theorem 4.11. *Let $\text{sim}_{p,e}(c_1, c_2) = \mu \in (0, 1)$ be the true functional similarity. We define the Signal-to-Noise Ratio (SNR) of an estimator \widehat{X} as $\text{SNR}(\widehat{X}) := (\mathbb{E}[\widehat{X}])^2 / \text{Var}(\widehat{X})$. For $m \geq 1$, the SNR of the smooth estimator dominates the sharp estimator by a factor of at least m^2 :*

$$\text{SNR}(\widehat{\text{sim}}_{p,e;m}) / \text{SNR}(\widehat{\text{sim}}_{p,e;m}^\infty) \geq m(1/\mu)^{m-1} \cdot \frac{1-\mu^m}{1-\mu} \geq m^2$$

Proof. Let $Z := \widehat{\text{sim}}_{p,e;1}(c_1, c_2 | e)$ be the random variable representing the similarity score on a single test suite, i.e., $Z \in [0, 1]$ and $\mathbb{E}[Z] = \mu \in (0, 1)$. The smooth estimator is the sample mean of m i.i.d. draws of Z . Its SNR depends on the variance of Z :

$$\text{SNR}(\widehat{\text{sim}}_{p,e;m}) = \frac{\mathbb{E}[\widehat{\text{sim}}_{p,e;m}]^2}{\text{Var}(\widehat{\text{sim}}_{p,e;m})} = \frac{\mu^2}{\text{Var}(Z)/m} = \frac{m\mu^2}{\text{Var}(Z)}.$$

Since Z is bounded in $[0, 1]$, $\text{Var}(Z) = \mathbb{E}[Z^2] - \mu^2 \leq \mathbb{E}[Z] - \mu^2 = \mu(1 - \mu)$. Thus:

$$\text{SNR}(\widehat{\text{sim}}_{p,e;m}) \geq \frac{m\mu^2}{\mu(1 - \mu)} = \frac{m\mu}{1 - \mu}.$$

The sharp estimator is an indicator that is 1 if and only if all sampled suites are perfect matches, i.e., $\widehat{\text{sim}}_{p,e;m}^\infty = \prod_{j=1}^m \mathbb{1}_{Z_j=1}$. Consequently, it is a Bernoulli variable with parameter p_1^m , where $p_1 = \mathbb{P}[Z = 1]$. As a result,

$$\text{SNR}(\widehat{\text{sim}}_{p,e;m}^\infty) = \frac{(p_1^m)^2}{p_1^m(1 - p_1^m)} = \frac{p_1^m}{1 - p_1^m}.$$

Now, since $Z \geq 0$, $p_1 \leq \mathbb{E}[Z] = \mu$. Moreover, for $m \geq 1$, $f(x) = \frac{x}{1-x}$ and $g(x) = x^m$ are both monotonously increasing between 0 and 1. As a result,

$$\text{SNR}(\widehat{\text{sim}}_{p,e;m}^\infty) \leq \frac{\mu^m}{1 - \mu^m}.$$

Taking the ratio of the lower bound of the smooth SNR to the upper bound of the sharp SNR and applying the formula for a finite geometric series in reverse yields

$$\frac{\text{SNR}(\widehat{\text{sim}}_{p,e;m})}{\text{SNR}(\widehat{\text{sim}}_{p,e;m}^\infty)} \geq \frac{\frac{m\mu}{1-\mu}}{\frac{\mu^m}{1-\mu^m}} = \frac{m}{\mu^{m-1}} \frac{1-\mu^m}{1-\mu} = \frac{m}{\mu^{m-1}} \sum_{k=0}^{m-1} \mu^k = m \sum_{k=0}^{m-1} \mu^{k-(m-1)}.$$

Finally, we observe that since $\mu \in (0, 1)$, every term $\mu^{k-(m-1)} \geq 1$. As there are m such terms:

$$\frac{\text{SNR}(\widehat{\text{sim}}_{p,e;m})}{\text{SNR}(\widehat{\text{sim}}_{p,e;m}^\infty)} \geq m \cdot m = m^2.$$

\square

Proposition 4.13. Let $\text{Pass}@k(\{\mathcal{N}_{c_i}^\infty\}_{i=1}^k) := \mathbb{P}_{t \sim p}[\exists i \in \{1, \dots, k\} : R(c_i, t | e) = 1]$. Assume a code-test calibrated model $p(c, t)$ with well-specification (Assumption 4.14). Then $\text{Pass}@k$ is maximized by greedily selecting the k code classes $\{\mathcal{N}_c^\infty\}_{1:k}$ with largest $p(\mathcal{N}_c^\infty)$.

Proof. Let $S = \{\mathcal{N}_{c_1}^\infty, \dots, \mathcal{N}_{c_k}^\infty\}$ be the set of k selected equivalence classes. We aim to maximize the expected recall:

$$\text{Pass}@k(S) = \mathbb{E}_t \left[\max_{\mathcal{N}_c^\infty \in S} \mathbb{1}_{R(c, t | e) = 1} \right] = \mathbb{P}_t [\exists \mathcal{N}_c^\infty \in S : R(c, t | e) = 1].$$

Define the success event for a class as $E_c := \{t \in \mathcal{V}^* : R(c, t | e) = 1\}$. Assumption 4.14 (Well-Specification) states that for any test suite t with $p(t) > 0$, there exists exactly one correct equivalence class. Consequently, for any two distinct classes $\mathcal{N}_{c_i}^\infty, \mathcal{N}_{c_j}^\infty \in S$, the intersection of their success events has zero measure ($\mathbb{P}[E_{c_i} \cap E_{c_j}] = 0$).

This mutual exclusivity allows us to decompose the probability of the union into a sum:

$$\text{Pass}@k(S) = \mathbb{P}_t \left[\bigcup_{\mathcal{N}_c^\infty \in S} E_c \right] = \sum_{\mathcal{N}_c^\infty \in S} \mathbb{P}_t[E_c].$$

Using the calibration assumption, we substitute the event probability with the model's measure: $\mathbb{P}_t[E_c] = p(\mathcal{N}_c^\infty)$. Thus:

$$\text{Pass}@k(S) = \sum_{\mathcal{N}_c^\infty \in S} p(\mathcal{N}_c^\infty).$$

Maximizing this sum subject to the constraint $|S| = k$ is a standard selection problem, for which the optimal solution is the greedy strategy: selecting the k classes with the largest probability mass $p(\mathcal{N}_c^\infty)$. \square

Theorem 5.1. Define the reward $r(x) := r_{obs}(x) + r_{hid}(x)$ for $r_{obs} \sim \mathcal{N}(\mu, \Sigma)$ and $\Sigma_{x,x} \leq 1 \forall x$ as well as finite $\mathbb{E}[r_{hid}]$. Let $x_{obs}^* \sim \mathbb{P}[x^* | r_{obs}]$ and $x_n \sim \mathbb{P}[x^* | \mathcal{H}_n]$ for $x^* := \arg \max_x r(x)$ and $\mathcal{H}_n := (x_i, y_i)_{i=1}^n$. Then

$$\mathbb{E}[\sum_{n=1}^T r(x_{obs}^*) - r(x_n)] \leq \beta \sqrt{C_\sigma T \gamma_T}.$$

Here, $\gamma_T := \max_{x_{1:T}} I(r_{obs}; y_{1:T})$ is the maximum information gain for observations $y_n := r_{obs}(x_n) + \eta_n$ with independent additive noise $\eta_n \sim \mathcal{N}(0, \sigma_n^2)$ of bounded amplitude $\sigma_n \leq \sigma$. $C_\sigma = 2/\ln(1 + \sigma^{-2})$ is a small constant depending on σ , and $\beta := 1 + \sqrt{2 \log(2 \cdot |r|) + 2}$.

Proof. Without loss of generality $\mathbb{E}[r_{hid}] = 0$, since nonzero expectations can be absorbed into μ , the expected value of r_{obs} . Given \mathcal{H}_n , define the independent copies $r'_{obs} \stackrel{d}{=} r_{obs}$ and $r'_{hid} \stackrel{d}{=} r''_{hid} \stackrel{d}{=} r_{hid}$. Then $x_{obs}^* := \arg \max_x r_{obs}(x) + r''_{hid}(x)$ and $x_n := \arg \max_x r'_{obs}(x) + r'_{hid}(x)$. Now, consider the regret decomposition

$$\mathbb{E}[r(x_{obs}^*) - r(x_n) | \mathcal{H}_n] = \mathbb{E}[r_{obs}(x_{obs}^*) - r_{obs}(x_n) | \mathcal{H}_n] = \mathbb{E}[r'_{obs}(x_n) - r_{obs}(x_n) | \mathcal{H}_n].$$

Here, we used that $r_{hid} \perp x_{obs}^*, x_n$ since x_{obs}^*, x_n are defined in terms of (observations of) r_{obs} and independent copies of r_{hid} , not r_{hid} itself. Moreover, we used that (w.l.o.g.) $\mathbb{E}[r_{hid}] = 0$ and that $r_{obs}(x_{obs}^*) \stackrel{d}{=} r'_{obs}(x_n)$ under any conditioning on the history \mathcal{H}_n , since both actions $x_{obs}^* := \arg \max_x r_{obs}(x) + r''_{hid}(x)$ and $x_n := \arg \max_x r'_{obs}(x) + r'_{hid}(x)$ follow exactly the same construction. Now, we take expectations with respect to \mathcal{H}_n and apply Lemma D.1 to obtain

$$\mathbb{E}[r(x_{obs}^*) - r(x_n)] \leq \beta \cdot \sqrt{\mathbb{E}[\sigma_{obs}(x_n)^2]}.$$

Applying Cauchy-Schwarz on the full regret sequence and conditioning on observations \mathcal{H}_n , then gives

$$\begin{aligned} \mathbb{E}[\sum_{n=1}^T r(x_{obs}^*) - r(x_n)] &\leq \beta \sum_{n=1}^T \sqrt{\mathbb{E}[\sigma_{obs}(x_n)^2]} \\ &\leq \beta \sqrt{T \sum_{n=1}^T \mathbb{E}[\sigma_{obs}(x_n)^2]} \leq \beta \sqrt{TC_\sigma \gamma_T}. \end{aligned}$$

Note the use of Lemma D.2 in the last step to bound $\sum_{n=1}^T \mathbb{E}[\sigma_{obs}(x_n)^2]$ with the maximal information gain γ_T . \square

D.1. Lemmas

Lemma D.1. Let $r, r' \sim \mathcal{N}(\mu, \Sigma)$ i.i.d. and let $x = f(r) \in \{1, \dots, |r|\}$ for an arbitrary function f . Then

$$\begin{aligned}\mathbb{E}[|r_x - \mu_x|] &\leq \sqrt{\mathbb{E}[\sigma_{\eta_x}^2] \cdot (2 \log(2|r|) + 2)} \text{ and} \\ \mathbb{E}[|r_x - r'_x|] &\leq \beta \cdot \sqrt{\mathbb{E}[\sigma_{\eta_x}^2]}.\end{aligned}$$

for $\beta := 1 + \sqrt{2 \log(2 \cdot |r|) + 2}$.

Proof. Note that $\forall z r_z - \mu_z = \sigma_z Z_z$ for $Z_z \sim \mathcal{N}(0, 1)$. Cauchy-Schwarz then gives, $\mathbb{E}[|r_x - \mu_x|] = \mathbb{E}[\sigma_{\eta_x} | Z_x] \leq \sqrt{\mathbb{E}[\sigma_{\eta_x}^2] \mathbb{E}[Z_x^2]}$. Now, $Z_x^2 \leq \max_{1 \leq j \leq n} Z_j^2$, so the tail integral formula for expectations with a union bound gives $\mathbb{E}[Z_x^2] \leq \mathbb{E}[\max_{1 \leq j \leq n} Z_j^2] \leq 2 \log(2|r|) + 2$. The first result then follows immediately. For the second result, apply the triangle inequality $\mathbb{E}[|r_x - r'_x|] \leq \mathbb{E}[|r_x - \mu_x|] + \mathbb{E}[|r'_x - \mu_x|]$, bound the first term as above, and the second term by $\sqrt{\mathbb{E}[\sigma_{\eta_x}^2]}$, using that $r' \perp x = f(r)$ and thus $\mathbb{E}[(Z'_x)^2] = 1$. \square

Lemma D.2. Let $r \sim \mathcal{N}(\mu, \Sigma)$ be a multivariate Gaussian with uniformly bounded standard deviations $\sigma_{r_x} \leq 1 \forall x$ that is consecutively evaluated at locations $L_T := (x_t)_{t=1}^T$ with observations $y_t = r_{x_t} + \eta_t$. The independent noise is distributed as $\eta_t \sim \mathcal{N}(0, \sigma_{x_t}^2)$ for $\sigma_x \leq \sigma \forall x$. Then the maximum information gain γ_T upper bounds the aggregated predictive variances at the evaluation locations, i.e.,

$$\gamma_T := \max_{L_T} I(y_{1:T}(L_T); r) \geq I(y_{1:T}; r) \geq \underbrace{\frac{\ln(1+\sigma^{-2})}{2}}_{=:1/C_\sigma} \sum_{t=1}^T \sigma_{r_{x_t}^t}^2.$$

Proof. The proof follows Menet et al. (2025b) which generalizes that of Srinivas et al. (2010) from homoscedastic to heteroscedastic noise. First, note that the expression on the right hand side is well-defined, because $\sigma_{r_{x_t}^t}$ only depends on the observation locations L_T , but not on the observed value. Next, note that $y_{1:T}|r$ is a multivariate normal with independent components of variance $\sigma_{x_1}^2, \dots, \sigma_{x_T}^2$, thus

$$\begin{aligned}I(y_{1:T}; r) &= H[y_{1:T}] - H[y_{1:T}|r] \\ &= H[y_{1:T}] - \frac{1}{2} \sum_{t=1}^T \ln(2\pi e \sigma_{x_t}^2).\end{aligned}$$

Furthermore, one may decompose

$$\begin{aligned}H[y_{1:T}] &= H[y_{1:T-1}] + H[y_T|y_{1:T-1}] \\ &= H[y_{1:T-1}] + \frac{1}{2} \ln(2\pi e (\sigma_{x_T}^2 + \sigma_{r_{x_T}^{T-1}}^2)),\end{aligned}$$

using that $y_T|y_{1:T-1}$ is Gaussian with variance $\sigma_{x_T}^2 + \sigma_{r_{x_T}^{T-1}}^2$. Recursively expanding then results in

$$I(y_{1:T}; r) = \frac{1}{2} \sum_{t=1}^T \ln(1 + \sigma_{x_t}^{-2} \sigma_{r_{x_t}^{t-1}}^2).$$

Finally, by assumption $\sigma_{r_{x_t}^t} \in [0, 1]$, allowing to lower bound each summand

$$\sigma_{r_{x_t}^{t-1}}^2 \leq \frac{1}{2} \ln(1 + \sigma_{x_t}^{-2} \sigma_{r_{x_t}^{t-1}}^2) \underbrace{\frac{2}{\ln(1 + \sigma_{x_t}^{-2})}}_{=:C_{\sigma_{x_t}}}.$$

The lower bound follows from $g(\sigma_{r_{x_t}^{t-1}}^2) := \ln(1 + \sigma_{x_t}^{-2} \sigma_{r_{x_t}^{t-1}}^2) - \sigma_{r_{x_t}^{t-1}}^2 \ln(1 + \sigma_{x_t}^{-2}) \geq 0 \forall \sigma_{r_{x_t}^t} \in [0, 1]$, which in turn follows from $g(0) = 0$, $g(1) = 0$, and concavity of g . \square